Published in final edited form as:

Bone. 2009 May ; 44(5): 795–804. doi:10.1016/j.bone.2009.01.003.

Glutaredoxin 5 regulates osteoblast apoptosis by protecting against oxidative stress

Gabriel R. Linares[a,b], **Weirong Xing**[a,c], **Kristen E. Govoni**[a], **Shin-Tai Chen**[a,d,e], and **Subburaman Mohan**[a,b,c,d]

[a]Musculoskeletal Disease Center, Jerry L. Pettis Memorial Veterans Affairs Medical Center, Loma Linda, CA 92357, USA

[b]Department of Physiology, Loma Linda University, Loma Linda, CA 92357, USA

[c]Department of Medicine, Loma Linda University, Loma Linda, CA 92357, USA

[d]Department of Biochemistry, Loma Linda University, Loma Linda, CA 92357, USA

[e]Department of Microbiology, Loma Linda University, Loma Linda, CA 92357, USA

Abstract

There is now increasing evidence which suggests an important role for reactive oxygen species (ROS) in the pathogenesis of osteoporosis. However, little is known on the molecular components of the oxidative stress pathway or their functions in bone. In this study, we evaluated the role and mechanism of action of glutaredoxin (Grx) 5, a protein that is highly expressed in bone. Osteoblasts were transfected with Grx5 siRNA and treated with hydrogen peroxide (H_2O_2). Grx5 siRNA treatment increased apoptosis while Grx5 overexpression protected MC3T3-E1 cells against H_2O_2 induced apoptosis and ROS formation. Grx5 deficiency results in impaired biogenesis of Fe–S cluster in yeast. Accordingly, activity of mitochondrial aconitase, whose activity is dependent on Fe–S cluster, decreased in Grx5 siRNA treated cells. Since reduced formation of Fe–S cluster would lead to increased level of free iron, a competitive inhibitor of manganese superoxide dismutase (MnSOD), we measured MnSOD activity in Grx5 deficient osteoblasts and found MnSOD activity was significantly reduced. The consequence of long term inhibition of Grx5 on osteoblast apoptosis was evaluated using lentiviral shRNA technology. Grx5 shRNA cells exhibited higher caspase activity and cardiolipin oxidation in the presence of H_2O_2. MnSOD activity was rescued by the addition of $MnCl_2$ to Grx5 shRNA osteoblasts in the presence of H_2O_2. Our findings are consistent with the hypothesis that Grx5 is an important determinant of osteoblast apoptosis and acts via a molecular pathway that involves regulation of ROS production, cardiolipin oxidation, caspase activity, Fe–S cluster formation, and MnSOD activity.

Keywords

Glutaredoxin 5 (Grx5); Oxidative stress; Reactive oxygen; species (ROS); Osteoblasts; Apoptosis

*Corresponding author. Musculoskeletal Disease Center (151), Jerry L. Pettis Memorial Veterans Affairs Medical Center, 11201 Benton Street, Loma Linda, CA 92357, USA. Fax: +1 909 796 1680., Subburaman.Mohan@va.gov (S. Mohan).

Introduction

The formation of reactive oxygen species (ROS) is an inevitable consequence of being an aerobic organism. Normal byproducts of respiration includes hydrogen peroxide (H_2O_2), superoxide anion (O_2^-), and hydroxyl radical (OH^-) [1,2]. These ROS can also derive from external environmental factors such as redox active drugs, radiation, and heavy metals [1]. However, the majority of the ROS produced by cells can be attributed to the mitochondrial respiratory chain [1]. Oxidative stress occurs when the levels of oxidants are higher than the levels of reductants, thus overwhelming the system [3]. Cells have developed both non-enzymatic and enzymatic defense mechanisms to counteract the deleterious effects of oxidative stress by either detoxifying ROS or repairing ROS induced damage. Some non-enzymatic examples include vitamin C, vitamin E, ubiquinone, flavenoids, and glutathione (GSH), and some examples of enzymatic scavengers include catalase, glutathione peroxidase, thioredoxin, Cu/Zn superoxide dismutase (Cu/Zn SOD), Mn/superoxide dismutase (MnSOD), and glutaredoxins [4]. Without these defensive mechanisms, the production of ROS in the cell would be unabated and the overall viability of the cell and cellular macromolecules would be compromised.

Recently there is mounting evidence that oxidative stress poses detrimental effects on bone by depleting antioxidants, activating osteoclasts, inhibiting bone formation, and increasing the incidence of apoptosis [5–11]. For example, increased oxidative stress results in decreased bone mineral density in aged men and women [12] and elderly osteoporotic women displayed lower plasma levels of antioxidants compared to age-matched controls [5]. Postmenopausal osteoporotic women displayed higher levels of lipid peroxidation and decreased activity of antioxidant enzymes including catalase, superoxide dismutase, and glutathione peroxidase [13,14]. These accumulating data provide strong evidence implicating the harmful effects of oxidative stress in bone, thus warranting further investigation to fully understand the mechanisms.

Glutaredoxins (Grx) are glutathione dependent oxidoreductases that help maintain cellular redox homeostasis in the cell [15]. The glutaredoxin system consists of GSH, NADPH, and GSH reductase [16]. The mammalian system contains three known members of the glutaredoxin family Grx1, Grx2, and Grx5. Grx1 (12 kDa), a dithiol glutaredoxin, is localized mainly in the cytosol and is involved in general disulfide-dithiol exchanges, donation of electrons to ribonucleotide reductase, dehydroascorbate reduction, regulation of transcription factors, differentiation, and apoptosis [15,17–21]. Grx2 (16 kDa), a dithiol glutaredoxin, localizes to either the mitochondria or the nucleus. Grx2 is involved in protein deglutathionylation of mitochondrial complex I, prevention of cardiolipin oxidation and cytochrome c release, and reduction of low molecular weight compounds such as GSSG and CoA disulphide [16]. The recently discovered Grx5, a monothiol glutaredoxin, is hypothetically localized to the mitochondria. Most of what is known on Grx5 has come from studies inyeast. The loss of Grx5 in yeast leads to constitutive oxidative damage, sensitization to ROS, iron accumulation, and inactivation of iron–sulfur (Fe–S) cluster containing enzymes [22–24]. A recent study by Wingert et al. [25] in zebrafish showed that loss of Grx5 causes hypochromic anemia and severely inhibits the formation of Fe–S clusters.

Several studies have demonstrated the importance of glutaredoxins in protecting against apoptosis. For example, overexpression of Grx1 protected cells from glucose deprivation induced metabolic stress by regulating the redox state of apoptosis signaling kinase 1 (ASK1) [26]. Studies by Murata et al. [27] also provided evidence that Grx1 is a key player in protecting against oxidative stress. The overexpression of glutaredoxin protected cardiac myocytes from hydrogen peroxide induced oxidative stress [28]. Specifically, Grx1 protected the redox state of AKT, a survival kinase that inactivates pro-apoptotic proteins, from inactivation by hydrogen peroxide. Similar to Grx1, Grx2 has also been shown to protect against apoptosis. Overexpression of Grx2 decreased the susceptibility of HeLa cells to apoptosis induced by doxorubicin or 2-deoxy-D-glucose [29]. Another study showed that the knockdown of Grx2 using siRNA, sensitized HeLa cells to cell death triggered by oxidative stress inducing compounds such as doxorubicin and phenylarsine oxide [30]. Together these findings indicate that glutaredoxins play a crucial role in protection against apoptosis. Since Grx5 is highly expressed in osteoblasts and little is known about the role of Grx5 in mammalian cells, we investigated the biological role of Grx5 in osteoblasts. Based on what is known about Grx1 and Grx2 actions in other systems, we hypothesized that Grx5 protects osteoblasts from oxidative stress. The purpose of this study is to evaluate the cause and effect relationship between Grx5 expression and osteoblast apoptosis and determine the molecular pathway for Grx5 action in osteoblasts.

Materials and methods

Cell culture

MC3T3-E1 cells were grown in standard growth media consisting of α-MEM (Invitrogen, Carlsbad, CA) containing 10% calf serum (Atlanta Biologicals, Norcross, GA)+1% penicillin/streptomycin (Cambrex Bioscience, Walkersville, MD). Serum free media consisted of α-MEM+1% penicillin/streptomycin and cell culture treatments with cadmium chloride ($CdCl_2$), hydrogen peroxide (H_2O_2), tumor necrosis factor-α (TNF-α), and manganese chloride ($MnCl_2$) were made in α-MEM+0.1% BSA+1% penicillin/streptomycin. Murine bone marrow stromal cells (BMSCs) were isolated and differentiation was induced as previously described [31]. Osteoblasts were isolated from the calvaria of 6 day old C57BL/6J mice as previously described [52]. Osteocalcin expression was used to confirm *in vitro* differentiation of BMSCs into osteoblasts. H_2O_2, $CdCl_2$, and $MnCl_2$ were purchased from Sigma-Aldrich (St. Louis, MO). TNF-α was obtained from PeproTech Incorporated (Rocky Hill, NJ).

RNA isolation and extraction

RNA was extracted from C57BL/6J mice, MC3T3-E1 cells, and BMSCs using an RNeasy Mini kit (Qiagen, Valencia, CA) as previously described [31].

Gene expression analysis

Real time RT-PCR was conducted according to the protocol previously described [31] using a Stratagene Brilliant SYBRGreen master mix (Stratagene, La Jolla, CA) and an ABI Prism 7000 sequence detection system (Applied Biosystems, Foster City, CA). Gene specific primers (Integrated DNA Technologies, San Diego, CA) were used to amplify Grx1

(forward: 5'-AACAACACCAGTGCGATTCA-3', reverse: 5'-ATCTGCTTCAGCCGAGTCAT-3'), Grx2 (forward: 5'-GCTGGAATATGGC-AACCAGT-3', reverse: 5'-GATGAA CCAGAGGCAGCAAT-3'), and Grx5 (coding region—forward: 5'-CGCTGGTGAAGAAGGACAA-3', reverse: 5'-TGGTTGGCCAGTTGGAGTA-3' and 3' untranslated region—forward: 5'-ATGTCGCGATCCTGTATTGC-3', reverse: 5'-TCCTCT GTCCATCATTTC-CC-3'). Peptidylprolyl isomerase A (PPIA) was used as the endogenous control. Fold change was calculated according to the formula $2^{-\Delta\Delta CT}$.

Gene transfection

MC3T3-E1 cells were transiently transfected by electroporation using 1 μg negative control siRNA (Qiagen, Valencia, CA) or 1 μg Grx5 siRNA (Santa Cruz Biotechnology, Santa Cruz, CA) with siPORT siRNA electroporation buffer (Ambion, Austin, TX). Electroporation was performed as previously described [32]. MC3T3-E1 cells were also transduced with lentiviral shRNA to evaluate the long term effect of gene silencing. MC3T3-E1 cells were transduced with Mission® non-target shRNA control (Sigma-Aldrich, St. Louis, MO) transduction particles or four different Mission® Grx5 transduction particles (Grx5 shRNA 86–89) (Sigma-Aldrich, St. Louis, MO). The efficiency of the four Grx5 shRNAs was evaluated to determine which one provided the highest inhibition of Grx5. Cells were seeded at a density of 5000 cells/well in a 24-well plate (BD Biosciences, San Jose, CA) in α-MEM+10% calf serum+1% penicillin/streptomycin. The following day the media were changed and 8 μg/ml hexadimethrine bromide was added to the media to enhance infection efficiency. Cells were transduced four times (morning and evening) using a MOI of 10 over the course of two days. After the last transduction, cells were replenished with fresh standard growth media for 1 day. Cells were then re-plated in a 6-well plate (Falcon) and the antibiotic puromycin (10 μg/ml) (Sigma-Aldrich, St. Louis, MO) was used in cell culture media for three days to perform selection. Following selection with 10 μg/ml puromycin, cells were expanded in standard growth media.

Cloning of Grx5 into MLV vector

Grx5 was amplified by PCR using *Mus musculus* liver cDNA (50 ng) as a template. Cloning was accomplished using PCR selection kit—high fidelity (Invitrogen, Carlsbad, CA). The reaction mixture consisted of 5 μl of 10× Pfx50 PCR mix, 1 μl each of forward and reverse primers, 2.5 μl of 10 mM dNTPs, 32.5 μl of DNA water, 2.5 μl DMSO, and 0.5 μl Pfx50 DNA polymerase. The 5' end of the forward primer contains a Kozak consensus sequence that initiates protein translation and the 3' end of the reverse primer contains a synthetic FLAG epitope (underlined) at the C-terminus that allows for identification of the protein. The primer sequences are (5' to 3'): Grx5 forward: 5'-GGG TCG AC GCC ACC ATG AGC GCG TCC CTG AGC CGG GCG GC-3' and Grx5 reverse: 5'-CGC GGA TCC TCA CTT GTC GTC ATC GTC TTT GTA GTC CTT GGA GTC TTG GTC CTT CTC ATC TA-3'. Amplification was carried out at 95 °C for 10 min, 40 cycles at 95 °C for 15 s, 60 °C for 1 min, and 72 °C for 3 min using Pfx50 DNA polymerase (Invitrogen, Carlsbad, CA) for PCR cloning due to its high specificity and high fidelity. The PCR product was purified with GeneClean spin kit (Qbiogene, Carlsbad, CA) according to manufacturer's instructions and was then digested overnight at 37 °C with Bam HI and Sal I. The digested product was

purified from a gel using GeneClean spin kit. Finally the PCR product was subcloned into the corresponding restriction sites of the MLV expression vector [33]. All plasmids were transformed into *E. coli* XL1 BLUE cells and the plasmids were isolated using EndoFree® Plasmid Maxi (Qiagen, Valencia, CA). The Grx5 PCR product sequence was confirmed by DNA Lab at Arizona State University (Tempe, AZ).

MLV-based vector production and MLV transduction

VSV-G protein was used as the envelope for our MLV-based vector and the vectors were generated by transient transfection in 293T cells as previously described [33]. Briefly, a 10-cm plate of 293T cells was transfected with a mixture of 20 μg of retroviral expression vector (Grx5 or β-gal control vectors), 10 μg of MLV-GP expression vector, and 1 μg of VSV-G expression vector by $CaPO_4$ precipitation. The conditioned medium containing the viral vectors was collected 48 h after the transfection. The viral titer was determined by the end-point dilution assay for the marker gene (β-Gal) expression in HT1080 cells. MC3T3-E1 cells were transduced as previously described [33].

Western blot analysis

Equal amounts of protein (20 μg) were resolved on a 15% SDS polyacrylamide gel. Proteins were transferred to a 0.2 μM nitrocellulose membrane (BioRad, Hercules, CA) at 300 mA for 20 min at 4 °C. The membrane was blocked in 5% milk in TBST overnight with rotation at 4 °C. The following day, the membrane was probed with specific antibody to anti-Flag (1:5000) (Sigma-Aldrich, St. Louis, MO) for 1 h. After washing, the membrane was incubated with horseradish peroxidase conjugated anti-mouse antibody (1:10,000) (Sigma-Aldrich, St. Louis, MO) for 1 h and then washed. Detection of Grx5 was visualized using Super Signal West Pico Chemiluminescent Substrate (Pierce, Rockford, IL). After exposure to chemiluminescene, the same membrane was stripped and reprobed with anti-β-actin (Sigma-Aldrich, St. Louis, MO).

Determination of apoptosis

Trypan blue exclusion was performed on MC3T3-E1 cells in the presence of $CdCl_2$ or H_2O_2. Cells were seeded at a density of 800 cells/ well in a 96-well dish (BD Biosciences, San Jose, CA). The media were changed to serum free for 24 h and cells were treated with different doses of $CdCl_2$ or H_2O_2 for 48 h. The media were removed and cells were incubated with 0.4% Trypan blue (ICN Biomedicals, Inc, Irvine, CA) in PBS for 45 min at 37 °C with 5% CO_2. The percentage of dead cells was calculated by dividing the number of dead (blue) cells by the number of live (clear) cells in a given field. Data are representative of four random fields per well. *DNA fragmentation* was quanitated in MC3T3-E1 cells transfected with negative control siRNA or Grx5 siRNA. Cells were seeded at a density of 200,000 cells/well in a 6-well dish (BD Biosciences, San Jose, CA) and were harvested according to the manufacturer's protocol (Calbiochem, San Diego, CA). Briefly, samples were diluted 1:20 and the number of nucleosomes was determined by measuring the absorbance at dual wavelengths of 450/ 595 nm. The amount of protein was determined according to the method of Bradford [34]. *Annexin V stain* was performed on β-Gal control, Grx5 overexpressing cells, and MC3T3-E1 cells transfected with negative control siRNA or

Grx5 siRNA. Cells were seeded at a density of 20,000 cells/well in a 24-well dish (BD Biosciences, San Jose, CA) and were treated with 200 μM H_2O_2 for 6 h. The cells were washed 2 times with PBS and incubated with 5 μl Alexa Fluor 488 annexin V (Molecular Probes Invitrogen, Carlsbad, CA) in 1× binding buffer to detect phosphatidylserine (PS). Plates were covered with foil and gently rotated for 15 min on an orbital shaker. After incubation, the media were removed and cells were washed with PBS. Images were immediately taken using an Olympus IX70 and fluorescence was observed using the appropriate filters. *Caspase 3,7 activity* was measured using Caspase-Glo 3,7 assay (Promega, Madison, WI). Non-target shRNA control or Grx5 shRNA cells were plated at a density of 2000 cells/well in a 96-well dish. The following day the media were replaced with serum free media. Twenty-four hours later cells were treated with either 200 μM H_2O_2 or 20 ng/ml TNF-α. Caspase 3,7 activity was determined after a 30 min incubation by measuring luminescence with Synergy 2 (Biotek Instruments Incorporated, Winooski, VT) according to the manufacturer's protocol.

MultiTox-Fluor multiplex cytotoxicity assay

Non-target shRNA control or Grx5 shRNA cells were plated at a density of 2000 cells/well in a 96-well dish (BD Biosciences, San Jose, CA). The following day the media were replaced with serum free media. Twenty-four hours later cells were treated with 20 ng/ml TNF-α for 24 h. Cytotoxicity (Promega, Madison, WI) was determined as per the manufacturer's instructions.

ROS assay

β-Gal control or Grx5 overexpressing cells were plated at a density of 2000 cells/well in a 96-well dish. The following day the cells were rinsed with serum free media and 24 h later cells were incubated with 20μM 2',7'-dichlorofluorescin diacetate (DCF) (Sigma-Aldrich, St. Louis, MO) for 45 min at 37 °C with 5% CO_2. Following incubation, cells were treated with 500 μM H_2O_2 for 2 h. ROS levels were determined by measuring the fluorescent intensity in Synergy 2 at excitation wavelength 485 nm and emission wavelength 530 nm.

Enzymatic activities

The activity of aconitase and manganese superoxide dismutase (MnSOD) was measured in MC3T3-E1 cells transfected with negative control siRNA or Grx5 siRNA. Briefly, the aconitase reaction mixture consisted of 90 mM Tris–HCl pH 7.5, 20 mM DL-isocitrate, 1 mM sodium citrate, dH_2O, and protein in a final volume of 1 ml. The formation of cis-aconitate was recorded for 6 min at 25 °C in a spectrophotometer at 240 nm. MnSOD activity (Cayman Chemical, Ann Arbor, MI) was measured according to the manufacturer's protocol. Protein concentrations were determined using the BioRad protein assay reagent.

10-N-nonyl acridine orange (NAO)

Cardiolipin oxidation was assessed by staining with NAO (Invitrogen, Carlsbad, CA), a probe for mitochondrial cardiolipin. Non-target shRNA control or Grx5 shRNA cells were plated at a density of 2000 cells/well in a 96-well dish. The following day the media were replaced with serum free media. Twenty-four hours later cells were treated with 200 μM

H_2O_2 or 400 μM H_2O_2. Following treatment for 12 h, cells were rinsed twice with PBS and incubated in 5 μM NAO for 30 min in the dark at room temperature. Samples were rinsed twice with PBS and fluorescence was measured at excitation wavelength 495 nm and emission wavelength 519 nm using Synergy 2 (Biotek Instruments Incorporated, Winooski, VT).

Statistical analysis

Data are presented as mean±SEM (standard error of the mean) and were analyzed using Student's *T*-test, one-way, or two-way ANOVA (Statistica 6, Tulsa, OK). Post-hoc analysis was performed using Duncan's test.

Results

Characterization of glutaredoxin expression in mouse tissues and cells

Although Grx5 is expressed in multiple tissues, its expression is greatest in bone (Fig. 1A). Furthermore, Grx5 is expressed at a 7-fold and 25-fold higher level than Grx1 and Grx2 respectively in bone (Fig.1B). Grx5 expression was examined during *in vitro* differentiation of bone marrow stromal cells into osteoblasts. As shown in Fig. 1C, Grx5 was upregulated 2.8-fold at day 12. Basal expression of Grx5 was also examined in MC3T3-E1 cells and undifferentiated bone marrow stromal cells, and there was no difference in Grx5 expression between these two cell types (data not shown). These results indicate that Grx5 is highly expressed in bone and cells of osteoblast lineage.

Grx5 deficient cells are sensitized to H_2O_2 induced apoptosis

To determine if Grx function is important in osteoblasts, MC3T3-E1 cells were treated with different doses of $CdCl_2$, a known inhibitor of Grx activity [20,27,28,30], and the effect on cell death was examined by trypan blue exclusion. Treatment with $CdCl_2$ resulted in a dose dependent increase in death of MC3T3-E1 cells (2.5-fold increase at the 1 μM dose) (Fig. 2A). In addition, treatment with H_2O_2 resulted in a dose dependent increase in death of MC3T3-E1 cells (Fig. 2B). To verify that the observed biological effects of $CdCl_2$ on osteoblasts is caused by inhibition of Grx activity, Grx5 was specifically knocked down by transfecting MC3T3-E1 cells with Grx5 siRNA using electroporation [32]. Grx5 expression decreased by 80% ($P<0.05$) and 40% ($P<0.05$) at 24 and 72 h, respectively, following transfection with Grx5 siRNA compared to negative control siRNA (data not shown). Grx5 knockdown did not alter the expression of other Grx family members (data not shown), thus suggesting that Grx5 siRNA effect is target specific.

To test the hypothesis that Grx5 protects osteoblasts against oxidative stress induced apoptosis, Grx5 siRNA transfected cells were treated with H_2O_2, a known inducer of oxidative stress. The dose of H_2O_2, 200 μM, used in our experiments was selected based on published reports [10,51]. Grx5 siRNA transfected cells treated with H_2O_2 exhibited 2.7-fold higher number of annexin V positive cells in comparison to control siRNA cells treated with H_2O_2 (Fig. 2C). One of the hallmark features of apoptosis is DNA fragmentation. DNA fragmentation induced by H_2O_2 was 2.2-fold higher in Grx5 siRNA transfected cells

compared to control siRNA transfected cells (Fig. 2D). These results suggest that Grx5 may function to protect osteoblasts from oxidative stress induced apoptosis.

TNF-α treatment sensitizes Grx5 shRNA osteoblasts to apoptosis

Since Grx5 siRNA that was used for functional studies only blocked Grx5 expression transiently, we used lentiviral vector based shRNA strategy to evaluate the consequence of long term inhibition of Grx5 on osteoblast apoptosis. MC3T3-E1 cells were transduced with either Grx5 shRNA clones or non-target shRNA control. Grx5 expression decreased by 70% in Grx5 shRNA 86 in comparison to control shRNA (Fig. 3A). Therefore, long term and stable knockdown of Grx5 was established in MC3T3-E1 cells.

Prompted by evidence that Grx5 deficient cells treated with H_2O_2 are sensitized to apoptosis, we proceeded to evaluate the effects of TNF-α, a known inducer of cell death [35,36] on Grx5 shRNA cells. We found that 24 h treatment with 20 ng/ml TNF-α increased cytotoxicity in shRNA control cells, but cytoxicity was induced by more than 3.5-fold in Grx5 shRNA 86 treated cultures in comparison to shRNA control (Fig. 3B). These results demonstrate that TNF-α treatment increases cell death and that loss of Grx5 sensitizes osteoblasts to TNF-α induced cell death.

Grx5 overexpression protects against H_2O_2 induced apoptosis

Because Grx5 inhibition in the presence of oxidative stress resulted in heightened sensitivity to apoptosis, we sought to determine if the overexpression of Grx5 offered protection against apoptosis. Grx5 expression was 54-fold higher in MC3T3-E1 cells transduced with MLV-Grx5 compared to MLV β-Gal control (Fig. 4A) and Grx5 protein was detected at 16 kDa using Flag antibody in Grx5 overexpressing cells but not β-Gal control cells (Fig. 4B). Grx5 overexpressing and β-Gal control cells were treated with 200 μM H_2O_2 for 6 h and annexin V staining was performed. As expected, Grx5 overexpression decreased the H_2O_2 effect as evidenced by fewer (38% less) annexin V positive cells in comparison to control (Fig. 4C). We also evaluated the effect of Grx5 overexpression on DNA fragmentation in the presence of H_2O_2 and found that Grx5 overexpression decreased DNA fragmentation by 50% in comparison to β-Gal control (Fig. 4D).

Grx5 mediates H_2O_2 induced ROS generation

It is well known that stressors such as H_2O_2 can induce ROS production and that ROS is a key mediator of apoptosis [3,37]. To determine the molecular pathway by which Grx5 protects against oxidative stress induced apoptosis, we determined the amount of ROS generated in response to H_2O_2 treatment in Grx5 overexpressing cells and β-Gal control cells. ROS levels increased 65% in β-Gal control cells following 2 h treatment with 500 μM H_2O_2. Moreover, Grx5 overexpression decreased H_2O_2 induced ROS production by 57% (Fig. 5A). These data demonstrate that H_2O_2 treatment increases oxidative stress and that Grx5 may act by regulating the levels of ROS in osteoblasts. Based on the finding that Grx5 overexpression decreased ROS production, we next evaluated the effect of ROS on cardiolipin oxidation. Cardiolipin is a mitochondrial lipid and previous studies have shown that cardiolipin oxidation is associated with apoptosis [29,38]. Non-target shRNA control and Grx5 shRNA cells were treated with H_2O_2 for 12 h and the effect on cardiolipin

oxidation was examined. Cardiolipin oxidation was significantly higher in Grx5 deficient cells in comparison to non-target shRNA control cells at two different doses of H_2O_2 (Fig. 5B).

Grx5 deficient cells exhibit increased caspase 3,7 activation in the presence of H_2O_2 and TNF-α

To further investigate the molecular mechanism of Grx5 during oxidative stress induced apoptosis, we measured caspase 3,7 activity in non-target control shRNA and Grx5 shRNA cells since caspase dependent apoptosis is a major mechanism by which TNF-α and H_2O_2 induce apoptosis [39]. Cells were treated with H_2O_2 and TNF-α, and caspase activity was measured at different timepoints. Maximal caspase activity was observed at 12 h in the H_2O_2 treated cells and the caspase activity of Grx5 shRNA cells was 3.6-fold higher in comparison to non-target shRNA cells (Fig. 6A). In cells treated with TNF-α, maximal caspase activity was observed at 48 h and Grx5 shRNA cells displayed a 2.3-fold higher caspase activity than non-target control shRNA cells (Fig. 6B). To confirm our results in MC3T3-E1 cells, caspase activity was also evaluated in primary calvaria osteoblasts transfected with Grx5 siRNA in the presence or absence of TNF-α for 48 h. As shown in Fig. 6C, Grx5 deficient calvaria osteoblasts exhibited higher caspase activity in comparison to control siRNA cells with or without TNF-α. Therefore, these data provide further evidence that Grx5 is important in regulating osteoblast apoptosis.

Grx5 siRNA treatment decreases aconitase and MnSOD activity

Previous studies in yeast have shown that Grx5 deficiency results in impaired biogenesis of Fe–S cluster, a critical cofactor for a large number of regulatory proteins [22,24,40–42]. The activity of aconitase, an Fe–S cluster dependent enzyme, was evaluated in Grx5 deficient cells. Aconitase activity decreased by 37% in Grx5 siRNA treated cells (Fig. 7A). Since reduced formation of Fe–S cluster would lead to increased level of free iron, a competitive inhibitor of MnSOD, MnSOD activity was measured in Grx5 deficient and control osteoblasts. As shown in Fig. 7B, Grx5 deficiency led to a 56% reduction in MnSOD activity. Inhibition of Grx5 did not alter aconitase or MnSOD gene expression (data not shown). These results suggest that Grx5 is a regulator of Fe–S cluster formation and may be involved in regulating the activities of aconitase and MnSOD in osteoblasts.

Previous studies have demonstrated that $MnCl_2$ increases SOD activity by competing with free iron in the active site [43–45]. To test our proposed model that Grx5 regulates SOD activity in osteoblasts by decreasing free iron levels, non-target shRNA control and Grx5 shRNA cells were treated with H_2O_2 in the presence of $MnCl_2$, and the effect on caspase activity was measured. We predicted that if loss of Grx5 decreased MnSOD activity by iron replacing Mn in the active site, then addition of excess Mn should rescue MnSOD activity. As expected, treatment with H_2O_2 alone increased caspase activity in both non-target shRNA control and Grx5 shRNA cells. Furthermore, H_2O_2 induced increase of caspase activity was significantly attenuated in the presence of $MnCl_2$ and Grx5 deficient cells were rescued from apoptosis (Fig. 7C). Therefore, these data provide evidence that Grx5 modulation of H_2O_2 induced apoptosis in osteoblasts is mediated in part by SOD activity.

Discussion

Although previous studies have shown that Grx1 and Grx2 regulate apoptosis [21,27,30,46], nothing was known about Grx5 function in any mammalian cell type. In this study we have provided the first direct evidence that Grx5 is important in regulating apoptosis in mammalian cells. Overexpression of Grx5 protected osteoblasts from apoptosis as evidenced by fewer annexin V positive cells and decreased DNA fragmentation. Inhibition of Grx5 augmented apoptosis as demonstrated by increased annexin V staining, DNA fragmentation, and caspase activity. Thus, all three members of Grx family seem to be involved in protecting cells against oxidative stress induced apoptosis.

Increased ROS production is an important mechanism for regulating apoptosis. For instance, the oxidation of cardiolipin, a mitochondrial lipid, results in cytochrome c release and activation of the apoptotic cascade [29]. Cardiolipin oxidation was higher in Grx5 deficient cells in the presence of H_2O_2 and this finding was consistent with increased markers for apoptosis in Grx5 deficient cells. Therefore elaborate antioxidant defense systems are in place to combat ROS. In MC3T3-E1 cells, we determined that Grx5 overexpression attenuated ROS production in the presence of H_2O_2. The regulation of ROS production in osteoblasts by Grx5 is in agreement with findings in yeast and plants [23,47], thus suggesting that the role of Grx5 in protecting against oxidative stress is conserved across multiple species. If Grx5 is the major antioxidant defense system in osteoblasts, we would then expect that loss of Grx5 to cause a large increase in ROS production and apoptosis. However, our data demonstrates that differences in ROS production and caspase activity in Grx5 deficient cells become manifested only in the presence of ROS inducers but not under basal conditions. One potential explanation for this observation is that multiple defense mechanisms may operate to protect cells during oxidative stress, since several antioxidant and enzymatic antioxidant systems are located in different parts of the cell. When one of these components is disrupted, redundancy enables another component to compensate. As a result, knockdown of Grx5 alone does not produce a drastic effect due to redundancy unless cells are exposed to higher oxidative stress.

In terms of mechanism by which Grx5 acts, studies by Rodrigues-Manzaneque et al. [24] have shown that Grx5 deficiency in yeast impairs the biogenesis of Fe–S cluster formation. Fe–S clusters are involved in electron transfer in oxidative phosphorylation of respiratory chain, stabilization of protein structure, citric acid cycle, and redox regulation [40,48]. Since the formation of Fe–S clusters is involved in a variety of complex cellular functions, disruption of Fe–S clusters can affect many components of the cell. Aconitase is a Fe–S cluster enzyme which plays an important role in the Krebs cycle. Inhibition of aconitase can have adverse affects on the Krebs cycle leading to impairment in energy production. Since Grx5 deficiency in yeast resulted in decreased aconitase activity, we examined the activity in osteoblasts and found that aconitase activity decreased in Grx5 siRNA transfected cells. This is in line with other studies that also reported decreased aconitase activity in the absence of Grx5 [25,42].

Inactivation of Fe–S clusters results in the release of free iron and an increase in free iron can be harmful to cells. It is well known that ROS is a normal byproduct of respiration, in

particular H_2O_2. Free Fe^{2+} can react with H_2O_2 to produce hydroxyl radical which is known as the Fenton reaction. The hydroxyl radical is highly reactive and can cause extensive oxidative damage to protein, lipids, and DNA. We hypothesized that inhibition of Grx5 would lead to decreased formation of FeS clusters and therefore intracellular levels of iron would be increased. Although we did not directly measure levels of iron in this study, it is known that increased levels of free iron inhibits MnSOD activity. Accordingly we observed that MnSOD activity was reduced in Grx5 siRNA cells. This is in agreement with the published results from Yang et al. [44] who observed that μgrx5 mutants (*Saccharomyces cerevisiae*) accumulated iron and exhibited decreased SOD activity and by Camaschella et al., [42] who noted that Grx5 deficient patients exhibited iron overload and anemia. MnSOD is a key mitochondrial enzyme in scavenging ROS. Mice expressing mutant SOD exhibited high ROS production and subsequent damage to mitochondria lipid and proteins [49]. MnSOD knockout mice exhibit increased lipid peroxidation [50]. Reduced activity of MnSOD would further exacerbate ROS production and apoptosis. We further tested this notion by treating cells simultaneously with $MnCl_2$ and H_2O_2 to determine if Grx5 deficient cells could be rescued from apoptosis. Consequently, $MnCl_2$ (an inducer of SOD activity) was able to rescue cells from apoptosis. Consistent with these results is the observation that Grx5 inhibition reduces MnSOD activity which cripples antioxidant defenses. Therefore it is important to maintain the integrity of Fe–S clusters because Grx5 acts to sequester free iron, thus alleviating stress and decreasing the opportunity for Fe^{2+} to react with H_2O_2 and form highly reactive superoxide radical.

In conclusion, we have demonstrated that Grx5 protects osteoblasts from oxidative stress induced apoptosis. The protective ability of Grx5 on apoptosis appears to be due to its ability to regulate ROS production, cardiolipin oxidation, caspase activity, Fe–S cluster formation, and MnSOD activity (Fig. 8). Therefore, our findings support the contention that Grx5 is an important mediator of osteoblast cell functions which acts as a scavenger of ROS and thereby attenuates its harmful effects by protecting against oxidative stress induced apoptosis. Our future studies will examine the relative contribution of Grx5 deficiency in the pathogenesis of bone loss under conditions of oxidative stress.

Acknowledgments

The authors would like to thank Thien Nguyen, Catrina Alarcon, Qianwei Tan, and Joe Rung-Aroon for their expert technical assistance. This work was supported by NIH grants R01AR31062, 1F31AR056204, and 5R25GM060507 (Loma Linda University-NIH Initiative for Minority Students Program). All work was performed with the facilities provided by the Department of Veterans Affairs.

References

1. Cabiscol E, Piulats E, Echave P, Herrero E, Ros J. Oxidative stress promotes specific protein damage in *Saccharomyces cerevisiae*. J Biol Chem. 2000; 275:27393–8. [PubMed: 10852912]
2. Karihtala P, Soini Y. Reactive oxygen species and antioxidant mechanisms in human tissues and their relation to malignancies. APMIS. 2007; 115:81–103. [PubMed: 17295675]
3. Ott M, Gogvadze V, Orrenius S, Zhivotovsky B. Mitochondria, oxidative stress and cell death. Apoptosis. 2007; 12:913–22. [PubMed: 17453160]
4. Martindale J, Holbrook N. Cellular response to oxidative stress: signaling for suicide and survival. J Cell Physiol. 2002; 192:1–15. [PubMed: 12115731]

5. Maggio D, Barabani M, Pierandrei M, Polidori M, Catani M, Mecocci P, Senin U, Pacifici R, Cherubini A. Marked decrease in plasma antioxidants in aged osteoporotic women: results of a cross-sectional study. J Clin Endocrinol Metab. 2003; 88:1523–7. [PubMed: 12679433]

6. Lean J, Davies J, Fuller K, Jagger C, Kirstein B, Partington G, Urry Z, Chambers T. A crucial role for thiol antioxidants in estrogen-deficiency bone loss. J Clin Invest. 2003; 112:915–23. [PubMed: 12975476]

7. Garrett I, Boyce B, Oreffo R, Bonewald L, Poser J, Mundy G. Oxygen-derived free radicals stimulate osteoclastic bone resorption in rodent bone in vitro and in vivo. J Clin Invest. 1990; 85:632–9. [PubMed: 2312718]

8. Liu A, Zhang Z, Zhu B, Liao Z, Liu Z. Metallothionein protects bone marrow stromal cells against hydrogen peroxide-induced inhibition of osteoblastic differentiation. Cell Biol Int. 2004; 28:905–11. [PubMed: 15566960]

9. Mody N, Parhami F, Sarafian T, Demer L. Oxidative stress modulates osteoblastic differentiation of vascular and bone cells. Free Radic Biol Med. 2001; 31:509–19. [PubMed: 11498284]

10. Park B, Yoo C, Kim H, Kwon C, Kim Y. Role of mitogen-activated protein kinases in hydrogen peroxide-induced cell death in osteoblastic cells. Toxicology. 2005; 215:115–25. [PubMed: 16125295]

11. Manolagas S, Almeida M. Gone with the Wnts: beta-catenin, T-cell factor, forkhead box O, and oxidative stress in age-dependent diseases of bone, lipid, and glucose metabolism. Mol Endocrinol. 2007; 21:2605–14. [PubMed: 17622581]

12. Basu S, Michaëlsson K, Olofsson H, Johansson S, Melhus H. Association between oxidative stress and bone mineral density. Biochem Biophys Res Commun. 2001; 288:275–9. [PubMed: 11594785]

13. Ozgocmen S, Kaya H, Fadillioglu E, Aydogan R, Yilmaz Z. Role of antioxidant systems, lipid peroxidation, and nitric oxide in postmenopausal osteoporosis. Mol Cell Biochem. 2007; 295:45–52. [PubMed: 16841180]

14. Sontakke A, Tare R. A duality in the roles of reactive oxygen species with respect to bone metabolism. Clin Chim Acta. 2002; 318:145–8. [PubMed: 11880125]

15. Holmgren A. Thioredoxin and glutaredoxin systems. J Biol Chem. 1989; 264:13963–6. [PubMed: 2668278]

16. Holmgren A, Johansson C, Berndt C, Lönn M, Hudemann C, Lillig C. Thiol redox control via thioredoxin and glutaredoxin systems. Biochem Soc Trans. 2005; 33:1375–7. [PubMed: 16246122]

17. Wells W, Xu D, Yang Y, Rocque P. Mammalian thioltransferase (glutaredoxin) and protein disulfide isomerase have dehydroascorbate reductase activity. J Biol Chem. 1990; 265:15361–4. [PubMed: 2394726]

18. Takashima Y, Hirota K, Nakamura H, Nakamura T, Akiyama K, Cheng F, Maeda M, Yodoi J. Differential expression of glutaredoxin and thioredoxin during monocytic differentiation. Immunol Lett. 1999; 68:397–401. [PubMed: 10424449]

19. Bandyopadhyay S, Starke D, Mieyal J, Gronostajski R. Thioltransferase (gluta-redoxin) reactivates the DNA-binding activity of oxidation-inactivated nuclear factor I. J Biol Chem. 1998; 273:392–7. [PubMed: 9417094]

20. Chrestensen C, Starke D, Mieyal J. Acute cadmium exposure inactivates thioltransferase (Glutaredoxin), inhibits intracellular reduction of protein-glutathionyl-mixed disulfides, and initiates apoptosis. J Biol Chem. 2000; 275:26556–65. [PubMed: 10854441]

21. Daily D, Vlamis-Gardikas A, Offen D, Mittelman L, Melamed E, Holmgren A, Barzilai A. Glutaredoxin protects cerebellar granule neurons from dopamine-induced apoptosis by activating NF-kappa B via Ref-1. J Biol Chem. 2001; 276:1335–44. [PubMed: 11035035]

22. Alves R, Herrero E, Sorribas A. Predictive reconstruction of the mitochondrial iron–sulfur cluster assembly metabolism. II. Role of glutaredoxin Grx5. Proteins. 2004; 57:481–92. [PubMed: 15382238]

23. Rodríguez-Manzaneque M, Ros J, Cabiscol E, Sorribas A, Herrero E. Grx5 glutaredoxin plays a central role in protection against protein oxidative damage in *Saccharomyces cerevisiae*. Mol Cell Biol. 1999; 19:8180–90. [PubMed: 10567543]

24. Rodríguez-Manzaneque M, Tamarit J, Bellí G, Ros J, Herrero E. Grx5 is a mitochondrial glutaredoxin required for the activity of iron/sulfur enzymes. Mol Biol Cell. 2002; 13:1109–21. [PubMed: 11950925]
25. Wingert R, Galloway J, Barut B, Foott H, Fraenkel P, Axe J, Weber G, Dooley K, Davidson A, Schmid B, Schmidt B, Paw B, Shaw G, Kingsley P, Palis J, Schubert H, Chen O, Kaplan J, Zon L. Deficiency of glutaredoxin 5 reveals Fe–S clusters are required for vertebrate haem synthesis. Nature. 2005; 436:1035–9. [PubMed: 16110529]
26. Song J, Lee Y. Differential role of glutaredoxin and thioredoxin in metabolic oxidative stress-induced activation of apoptosis signal-regulating kinase 1. Biochem J. 2003; 373:845–53. [PubMed: 12723971]
27. Murata H, Ihara Y, Nakamura H, Yodoi J, Sumikawa K, Kondo T. Glutaredoxin exerts an antiapoptotic effect by regulating the redox state of Akt. J Biol Chem. 2003; 278:50226–33. [PubMed: 14522978]
28. Urata Y, Ihara Y, Murata H, Goto S, Koji T, Yodoi J, Inoue S, Kondo T. 17Beta-estradiol protects against oxidative stress-induced cell death through the glutathione/ glutaredoxin-dependent redox regulation of Akt in myocardiac H9c2 cells. J Biol Chem. 2006; 281:13092–102. [PubMed: 16549430]
29. Enoksson M, Fernandes A, Prast S, Lillig C, Holmgren A, Orrenius S. Overexpression of glutaredoxin 2 attenuates apoptosis by preventing cytochrome c release. Biochem Biophys Res Commun. 2005; 327:774–9. [PubMed: 15649413]
30. Lillig C, Lönn M, Enoksson M, Fernandes A, Holmgren A. Short interfering RNA-mediated silencing of glutaredoxin 2 increases the sensitivity of HeLa cells toward doxorubicin and phenylarsine oxide. Proc Natl Acad Sci U S A. 2004; 101:13227–32. [PubMed: 15328416]
31. Govoni K, Lee S, Chadwick R, Yu H, Kasukawa Y, Baylink D, Mohan S. Whole genome microarray analysis of growth hormone-induced gene expression in bone: T-box3, a novel transcription factor, regulates osteoblast proliferation. Am J Physiol, Endocrinol Metab. 2006; 291:E128–136. [PubMed: 16464905]
32. Xing W, Singgih A, Kapoor A, Alarcon C, Baylink D, Mohan S. Nuclear factor-E2-related factor-1 mediates ascorbic acid induction of osterix expression via interaction with antioxidant-responsive element in bone cells. J Biol Chem. 2007; 282:22052–61. [PubMed: 17510056]
33. Peng H, Chen S, Wergedal J, Polo J, Yee J, Lau K, Baylink D. Development of an MFG-based retroviral vector system for secretion of high levels of functionally active human BMP4. Mol Ther. 2001; 4:95–104. [PubMed: 11482980]
34. Bradford M. A rapid and sensitive method for the quantitation of microgram quantities of protein utilizing the principle of protein-dye binding. Anal Biochem. 1976; 72:248–54. [PubMed: 942051]
35. Chua C, Chua B, Chen Z, Landy C, Hamdy R. TGF-beta1 inhibits multiple caspases induced by TNF-alpha in murine osteoblastic MC3T3-E1 cells. Biochim Biophys Acta. 2002; 1593:1–8. [PubMed: 12431778]
36. Suh K, Koh G, Park C, Woo J, Kim S, Kim J, Park I, Kim Y. Soybean isoflavones inhibit tumor necrosis factor-alpha-induced apoptosis and the production of interleukin-6 and prostaglandin E2 in osteoblastic cells. Phytochemistry. 2003; 63:209–15. [PubMed: 12711143]
37. Simon H, Haj-Yehia A, Levi-Schaffer F. Role of reactive oxygen species (ROS) in apoptosis induction. Apoptosis. 2000; 5:415–8. [PubMed: 11256882]
38. Wiseman D, Wells S, Hubbard M, Welker J, Black S. Alterations in zinc homeostasis underlie endothelial cell death induced by oxidative stress from acute exposure to hydrogen peroxide. Am J Physiol, Lung Cell Mol Physiol. 2007; 292:L165–177. [PubMed: 16936243]
39. Byun C, Koh J, Kim D, Park S, Lee K, Kim G. Alpha-lipoic acid inhibits TNF-alpha-induced apoptosis in human bone marrow stromal cells. J Bone Miner Res. 2005; 20:1125–35. [PubMed: 15940365]
40. Lill R, Dutkiewicz R, Elsässer H, Hausmann A, Netz D, Pierik A, Stehling O, Urzica E, Mühlenhoff U. Mechanisms of iron–sulfur protein maturation in mitochondria, cytosol and nucleus of eukaryotes. Biochim Biophys Acta. 2006; 1763:652–67. [PubMed: 16843540]

41. Molina-Navarro M, Casas C, Piedrafita L, Bellí G, Herrero E. Prokaryotic and eukaryotic monothiol glutaredoxins are able to perform the functions of Grx5 in the biogenesis of Fe/S clusters in yeast mitochondria. FEBS Lett. 2006; 580:2273–80. [PubMed: 16566929]
42. Camaschella C, Campanella A, De Falco L, Boschetto L, Merlini R, Silvestri L, Levi S, Iolascon A. The human counterpart of zebrafish shiraz shows sideroblastic-like microcytic anemia and iron overload. Blood. 2007; 110:1353–8. [PubMed: 17485548]
43. Yamakura F, Kobayashi K, Furukawa S, Suzuki Y. In vitro preparation of iron-substituted human manganese superoxide dismutase: possible toxic properties for mitochondria. FreeRadic Biol Med. 2007; 43:423–30.
44. Yang M, Cobine P, Molik S, Naranuntarat A, Lill R, Winge D, Culotta V. The effects of mitochondrial iron homeostasis on cofactor specificity of superoxide dismutase 2. EMBO J. 2006; 25:1775–83. [PubMed: 16601688]
45. Beyer WJ, Fridovich I. In vivo competition between iron and manganese for occupancy of the active site region of the manganese-superoxide dismutase of Escherichia coli. J Biol Chem. 1991; 266:303–8. [PubMed: 1985901]
46. Nagy N, Malik G, Tosaki A, Ho Y, Maulik N, Das D. Overexpression of glutaredoxin-2 reduces myocardial cell death by preventing both apoptosis and necrosis. J Mol Cell Cardiol. 2008; 44:252–60. [PubMed: 18076901]
47. Cheng N, Liu J, Brock A, Nelson R, Hirschi K. AtGRXcp, an Arabidopsis chloroplastic glutaredoxin, is critical for protection against protein oxidative damage. J Biol Chem. 2006; 281:26280–8. [PubMed: 16829529]
48. Mühlenhoff U, Gerber J, Richhardt N, Lill R. Components involved in assembly and dislocation of iron–sulfur clusters on the scaffold protein Isu1p. EMBO J. 2003; 22:4815–25. [PubMed: 12970193]
49. Mattiazzi M, D'Aurelio M, Gajewski C, Martushova K, Kiaei M, Beal M, Manfredi G. Mutated human SOD1 causes dysfunction of oxidative phosphorylation in mitochondria of transgenic mice. J Biol Chem. 2002; 277:29626–33. [PubMed: 12050154]
50. Melov S, Coskun P, Patel M, Tuinstra R, Cottrell B, Jun A, Zastawny T, Dizdaroglu M, Goodman S, Huang T, Miziorko H, Epstein C, Wallace D. Mitochondrial disease in superoxide dismutase 2 mutant mice. Proc Natl Acad Sci U S A. 1999; 96:846–51. [PubMed: 9927656]
51. Fatokun A, Stone TW, Smith RA. Hydrogen peroxide-induce oxidative stress in MC3T3-E1 cells: the effects of glutamate and protection by purines. Bone. 2006; 39:542–51. [PubMed: 16616712]
52. Miyakoshi N, Richman C, Kasukawa Y, Linkhart TA, Baylink DJ, Mohan S. Evidence that IGF-binding protein-5 functions as a growth factor. J Clin Invest. 2001; 107:73–81. [PubMed: 11134182]

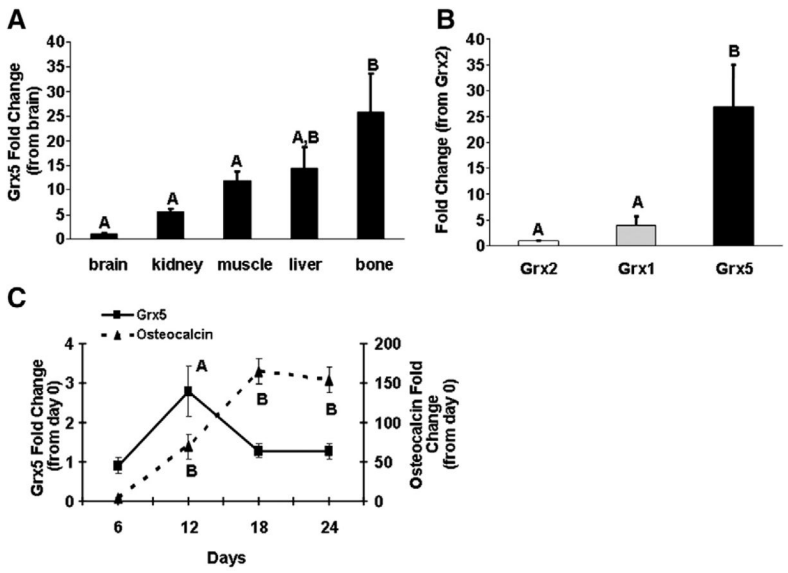

Fig. 1.

Glutaredoxin expression in mouse tissues and cells. (A) Grx5 expression in tissues of 8 week old C57BL/6J mice as determined by real time RT-PCR. Values are presented as mean ±SEM of 3 replicates. A,B: data with different letters indicate significant difference at $P<0.05$. Tissues with same letters are not statistically different. (B) Grx 1, 2, and 5 expression in the bones of 8 week old C57BL/6J mice as determined by real time RT-PCR. Values are presented as mean±SEM of 3 replicates. A,B: data with different letters indicate significant difference at $P<0.05$. Genes with same letters are not statistically different. (C) Grx5 expression during *in vitro* differentiation of bone marrow stromal cells into osteoblasts. RNA was extracted at days 0, 6,12,18, and 24. Differentiation of bone marrow stromal cells into osteoblasts was confirmed by osteocalcin expression. Values are presented as mean±SEM of 6 replicates. A=$P<0.01$ vs. day 0 (Grx5) and B=$P<0.05$ vs. day 0 (osteocalcin).

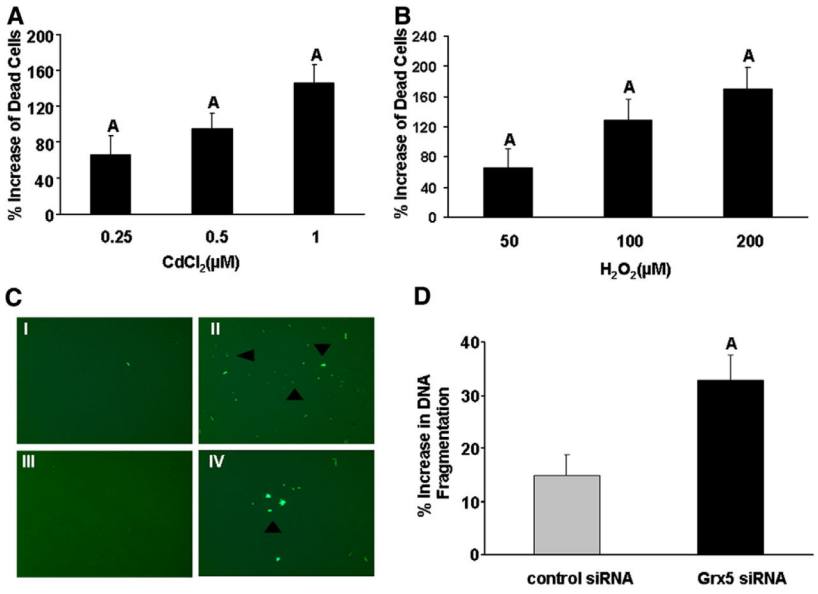

Fig. 2.

Inhibition of Grx5 augments cell death. Trypan blue exclusion of MC3T3-E1 cells treated with different doses of either $CdCl_2$ (A) or H_2O_2 (B) for 48 h. Values are presented as % increase from BSA treated control±SEM (n=8). A=P<0.05 vs. control. (C) Annexin V stain of MC3T3-E1 cells transfected with either control siRNA or Grx5 siRNA for 24 h. Cells were treated with 200 μM H_2O_2 for 6 h. Panels are representative of I) Grx5 siRNA-control, II) Grx5 siRNA-H_2O_2, III) control siRNA-control, and IV) control siRNA-H_2O_2. Annexin V positive cells (green) were visualized by fluorescent microscopy using an Olympus IX70. Images were taken at 40×magnification and arrowheads indicate apoptotic cells. (D) DNA fragmentation assay of MC3T3-E1 cells transfected with either control siRNA or Grx5 siRNA for 24 h and then treated with 200 μM H_2O_2 for 6 h. Values are expressed as % increase from corresponding BSA treated control±SEM (n=5). A=P<0.05 vs. control siRNA.

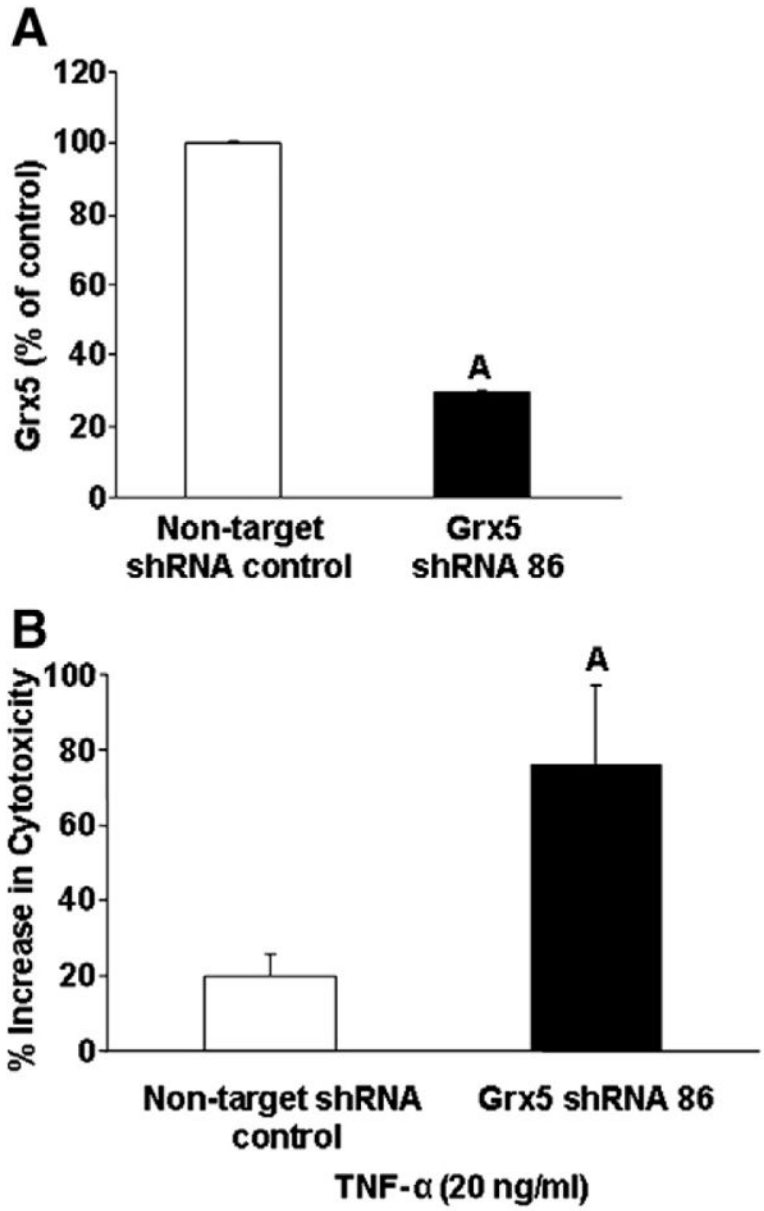

Fig. 3.

Lentiviral Grx5 shRNA transduction in MC3T3-E1 cells induces cytotoxicity in the presence of TNF-α. (A) Grx5 expression in MC3T3-E1 cells transduced with either non-target shRNA control or Grx5 shRNA 86 as determined by real time RT-PCR. Values are presented as mean±SEM of 4 replicates. A=P<0.01 vs. non-target shRNA control. (B) TNF-α induced cytotoxicity in non-target shRNA control or Grx5 shRNA 86. Cells were treated with either vehicle or 20 ng/ml TNF-α for 24 h. The number of dead cells was determined using MultiTox-Fluor multiplex cytotoxicity assay. Values are expressed as % increase from corresponding BSA treated control±SEM (n=6). Basal values (relative fluorescent units) of non-target shRNA control (98.0 RFU±8.17) and Grx5 shRNA 86 (148.50 RFU±19.44). A=P<0.05 vs. non-target shRNA control.

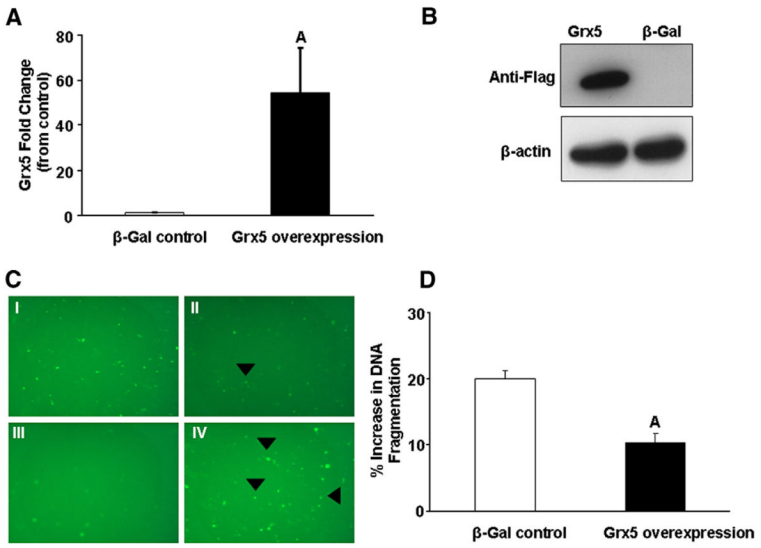

Fig. 4.

Grx5 overexpression attenuates H_2O_2 induced apoptosis in MC3T3-E1 cells. (A) Grx5 expression in β-Gal control and Grx5 overexpressing cells as determined by real time RT-PCR. Values are presented as mean±SEM of 3 replicates. A=P<0.01 vs. β-Gal control. (B) Detection of Grx5 protein (16 kDa). (C) Annexin V stain of β-Gal control and Grx5 overexpressing cells following treatment with 200 μM H_2O_2 for 6 h. Panels are representative of I) Grx5 overexpression-control, II) Grx5 overexpression-H_2O_2, III) β-Gal control– control, and IV) β-Gal control-H_2O_2. Images were taken at 40× magnification and arrowheads indicate apoptotic cells. (D) DNA fragmentation assay of β-Gal control and Grx5 overexpressing cells treated with 200 μM H_2O_2 for 6 h. Values are presented as % increase from corresponding BSA treated control±SEM (n =4). A= P < 0.05 vs. β-Gal control.

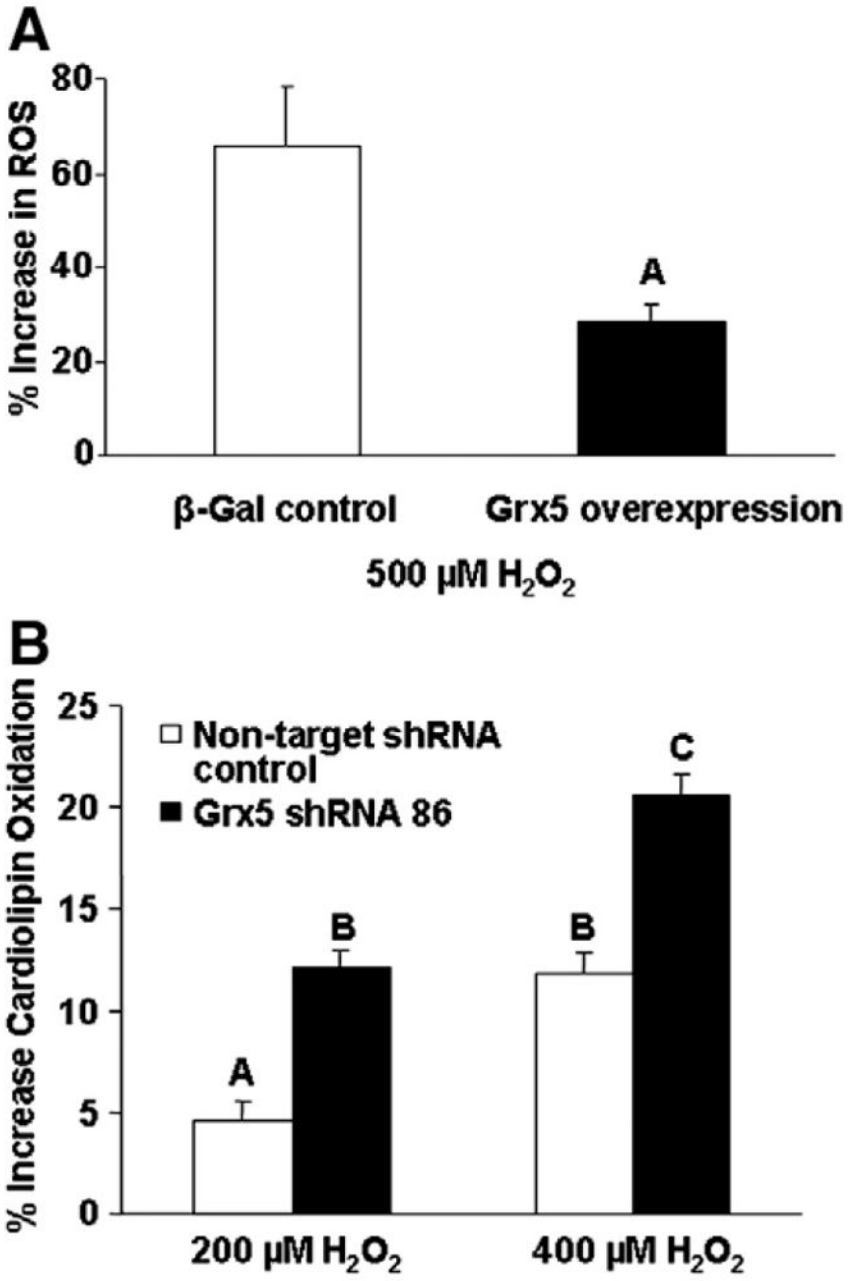

Fig. 5.

Effect of Grx5 overexpression or inhibition on H_2O_2 induced ROS generation in MC3T3-E1 cells. (A) ROS generation in β-Gal control or Grx5 overexpressing cells treated with 500 μM H_2O_2 for 2 h. Values are presented as % increase from corresponding BSA treated control± SEM (*n*=5). A= *P* <0.05 vs. β-Gal control. (B) Cardiolipin oxidation of Grx5 shRNA and non-target shRNA control cells following treatment with 200 μM H_2O_2 and 400 μM H_2O_2 for 12 h. Cardiolipin oxidation was measured using 5 μM NAO. Values are presented as % increase from corresponding BSA treated control±SEM (*n*=6–8). Basal values (relative fluorescent units) of non-target shRNA control (370.83 RFU±15.99) and Grx5 shRNA 86

(328.13 RFU±15.56). A, B, C: data with different letters indicate significant difference at $P<0.001$. Treatment groups with same letters are not statistically different.

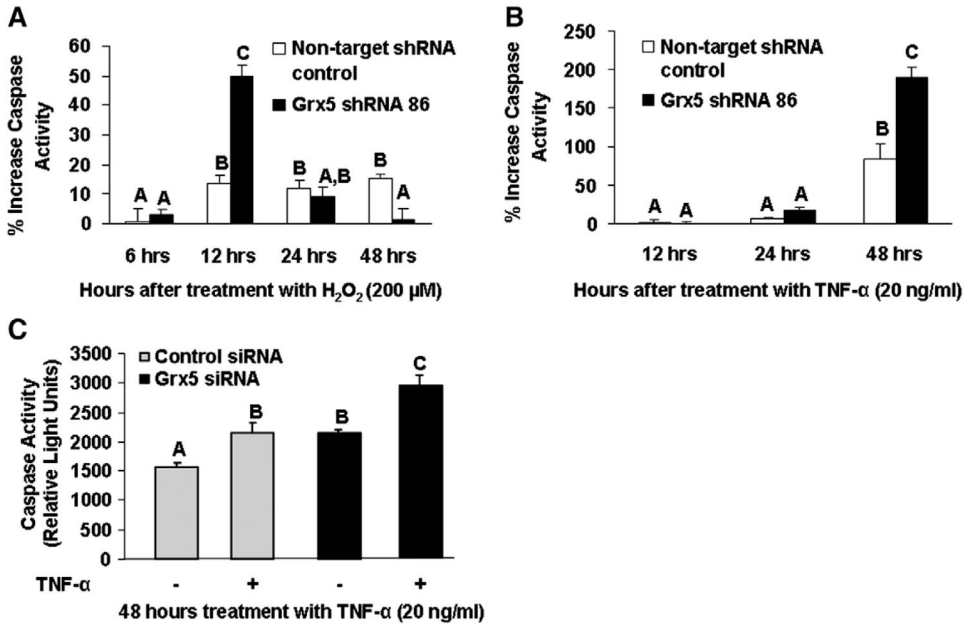

Fig. 6.

Grx5 deficient cells exhibit increased caspase 3,7 activity. Caspase 3,7 activity in non-target shRNA control or Grx5 shRNA following treatment with either (A) 200 μM H_2O_2 or (B) 20 ng/ml TNF-α. Caspase 3,7 activity was measured at the times indicated on the graph. Values are presented as % increase from corresponding BSA treated control±SEM (*n*=5–6). A,B,C: data with different letters indicate significant difference at $P<0.05$. Treatment groups with same letters are not statistically different. (C) Caspase 3,7 activity in primary calvaria osteoblasts transfected with control siRNA or Grx5 siRNA following treatment with TNF-α for 48 h. Values are presented as mean±SEM (*n*=5–6). A,B,C: data with different letters indicate significant difference at $P<0.01$. Treatment groups with same letters are not statistically different.

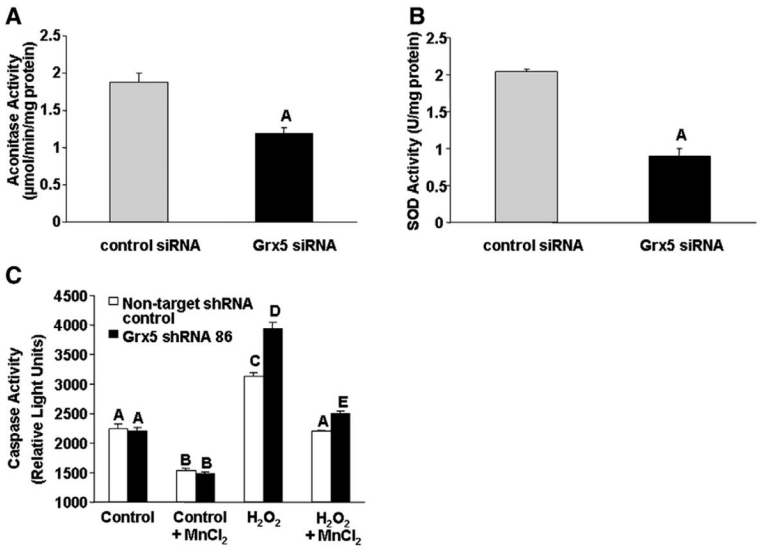

Fig. 7.

Grx5 siRNA treatment reduces the activities of aconitase and MnSOD. MC3T3-E1 cells were transfected with either control siRNA or Grx5 siRNA for 72 h. (A) Aconitase activity was measured following a 6 min incubation. A=P<0.01 vs. control siRNA. Values are presented as mean±SEM (n=3). (B) MnSOD activity was detected following a 20 min incubation. A=P<0.001 vs. control siRNA. Values are presented as mean±SEM (n=3). (C) Caspase 3,7 activity in non-target shRNA control and Grx5 shRNA cells following 12 h treatment with 200 μM H_2O_2 in the presence or absence of 200 μM $MnCl_2$. Cells were pretreated with $MnCl_2$ for 45 min prior to the addition of H_2O_2. Values are presented as mean ±SEM (n=6). A,B,C,D,E: data with different letters indicate significant difference at P<0.01. Treatment groups with same letters are not statistically different.

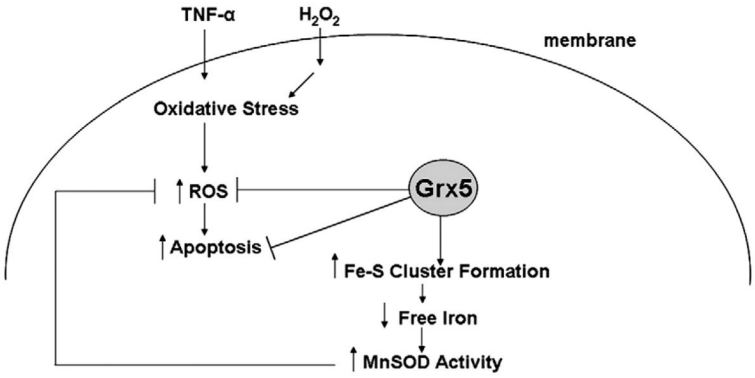

Fig. 8.

Proposed model for mechanism of Grx5 action. Grx5 protects osteoblasts against oxidative stress induced apoptosis by scavenging ROS and decreasing DNA fragmentation. Since Grx5 plays a role in Fe–S cluster formation, it regulates the activity of MnSOD (ROS scavenger).